



ChemComm

**A mononuclear, terminal titanium(III) imido**

Journal:	<i>ChemComm</i>
Manuscript ID	CC-COM-04-2023-001758.R1
Article Type:	Communication

SCHOLARONE™  
Manuscripts

## COMMUNICATION

## A mononuclear, terminal titanium(III) imido

Jacob S. Mohar,<sup>a</sup> Anders Reinholdt,<sup>a</sup> Taylor M. Keller,<sup>a</sup> Patrick J. Carroll,<sup>a</sup> Joshua Telser,<sup>b,\*</sup> and Daniel J. Mindiola<sup>a,\*</sup>Received 00th January 20xx,  
Accepted 00th January 20xx

DOI: 10.1039/x0xx00000x

We report the first mononuclear Ti<sup>III</sup> complex possessing a terminal imido ligand. Complex [Tp<sup>tBu,Me</sup>Ti(≡NSi(CH<sub>3</sub>)<sub>3</sub>)(THF)] (2) (Tp<sup>tBu,Me</sup> = hydridotris(3-tert-butyl-5-methylpyrazol-1-yl)borate) is prepared by reduction of [Tp<sup>tBu,Me</sup>Ti(≡NSi(CH<sub>3</sub>)<sub>3</sub>)(Cl)] (1) with KC<sub>8</sub> in high yield. The connectivity and metalloradical nature of 2 were confirmed by single crystal X-ray diffraction studies (scXRD), Q- and X-band EPR, UV-Vis and <sup>1</sup>H NMR spectroscopies. The d<sup>1</sup> complex [(Tp<sup>tBu,Me</sup>TiCl(OEt<sub>2</sub>))[B(C<sub>6</sub>F<sub>5</sub>)<sub>4</sub>] (3), was prepared to spectroscopically compare it to 2. Electrochemical studies of 1 and 2 reveal a reversible 1e<sup>-</sup> process, and chemical oxidants ClCPh<sub>3</sub> or ½ eq. XeF<sub>2</sub> react cleanly with 2 yielding 1 or the fluoride derivative [Tp<sup>tBu,Me</sup>Ti(≡NSi(CH<sub>3</sub>)<sub>3</sub>)(F)] (4), respectively, with the latter being fully characterized including a scXRD study.

Early transition metal (group III-VI) imidos (RN<sup>2-</sup>) have been studied extensively for the past 60 years due to their utility in stoichiometric<sup>1</sup> and catalytic reactions.<sup>2</sup> Specifically, titanium imidos have shown great utility in Ziegler-Natta polymerization,<sup>2b,3</sup> cycloaddition,<sup>4</sup> group transfer,<sup>1b,5</sup> hydroamination,<sup>5b,6</sup> C-H bond activation,<sup>7</sup> carboamination,<sup>8</sup> and hydrogenation reactions.<sup>7b,9</sup> The earliest reports of Ti<sup>IV</sup> imidos, by Bradley *et al.*, date back to 1963 followed by the first structural characterization of a polymeric Ti<sup>IV</sup> imido complex containing bridging imido and chloride ligands, [Ti{μ-NSi(CH<sub>3</sub>)<sub>3</sub>}(μ-Cl)Cl]<sub>n</sub>, reported by Alcock *et al.* in 1974.<sup>10</sup> Not until 1990 when Hill *et al.* reported a terminal, mononuclear Ti<sup>IV</sup> imido did two distinct classes of Ti imidos displaying either bridging or terminal coordination emerge.<sup>9b,11</sup> Both coordination modes of Ti imidos are dominated by diamagnetic, Ti<sup>IV</sup> centers. Terminal, mononuclear Ti<sup>III</sup> imidos have entirely eluded isolation despite being isoelectronic with the ubiquitous vanadyl ion, {V=O}<sup>2+</sup>, a system which helped establish the present-day understanding of metal-ligand multiple bonds and

redox-properties.<sup>9b,12</sup> Dinuclear Ti<sup>III</sup> imido systems, however, have been reported in both coordination modes. Cummins *et al.* showed the reduction of complex [(<sup>t</sup>Bu<sub>3</sub>SiNH)(THF)(R)Ti≡NSi<sup>t</sup>Bu<sub>3</sub>] (R = Me, <sup>t</sup>Bu) with H<sub>2</sub> yielded [(<sup>t</sup>Bu<sub>3</sub>SiNH)Ti{μ-NSi<sup>t</sup>Bu<sub>3</sub>}]<sub>2</sub>, Fig 1A, representing the first example of Ti<sub>2</sub><sup>III,III</sup> bridging imidos.<sup>7b</sup> Later, Bai *et al.* reported the ligand fragmentation product K<sub>2</sub>{[η<sup>2</sup>-ArNC(CH<sub>3</sub>)CHC(CH<sub>3</sub>)(ArN)Ti(μ-H)]<sub>2</sub> (Ar = 2,6-<sup>i</sup>Pr<sub>2</sub>C<sub>6</sub>H<sub>3</sub>, Fig 1B), representing a Ti<sub>2</sub><sup>III,III</sup> complex containing terminal imidos.<sup>13</sup> Other examples include the mixed valence Ti<sub>2</sub><sup>III,IV</sup> complex [CoCp<sub>2</sub>][(C<sub>5</sub>R<sub>5</sub>)Ti(Cl){μ-NAr}]<sub>2</sub> (R = H, Me; Ar = 3,5-(CF<sub>3</sub>)<sub>2</sub>C<sub>6</sub>H<sub>3</sub>) by Tsurugi *et al.* containing two bridging imidos (Fig 1C),<sup>14</sup> and, more recently, the Ti<sub>2</sub><sup>III,III</sup> complex [K(18-crown-6)(THF)<sub>2</sub>][(Nim<sup>Ar</sup>)(NAd)Ti(μ-NAd)<sub>2</sub>Ti(Nim<sup>Ar</sup>)(K)] (Nim<sup>Ar</sup> = 1,3-bis(Ar)imidazolin-2-iminato; Ar = 2,6-<sup>i</sup>Pr<sub>2</sub>C<sub>6</sub>H<sub>3</sub>; Ad = adamantyl) containing one terminal and two bridging imidos by Gómez-Torres, *et al.* (Fig 1D).<sup>15</sup> Inspired by these advances, and given our recent success in isolating a pseudo-tetrahedral Ti<sup>II</sup> center,<sup>16</sup> we sought to expand the chemistry of Ti imidos by synthesizing and fully characterizing a terminal, mononuclear Ti<sup>III</sup> imido and probing its electronic structure and redox properties.

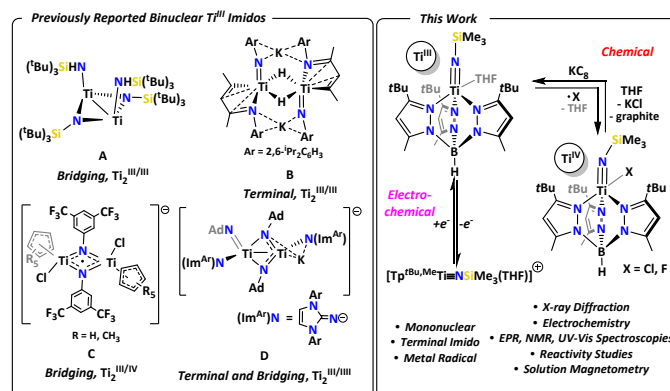
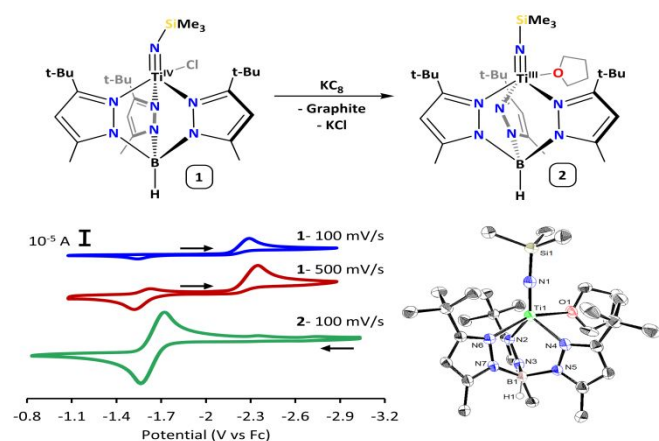


Fig 1: Left: Previous examples of isolated and structurally characterized dinuclear Ti<sup>III</sup> imido complexes A-D. Cations for C (CoCp<sub>2</sub><sup>+</sup>), and D (K(18-crown-6)(THF)<sub>2</sub><sup>+</sup>) are omitted for clarity. Right (this work): A mononuclear, terminal Ti<sup>III</sup> imido displaying redox reactivity.

<sup>a</sup> Department of Chemistry, University of Pennsylvania, 231 S 34<sup>th</sup> Street Philadelphia, Pennsylvania, United States

\*Corresponding Authors: mindiola@sas.upenn.edu; jtelsel@roosevelt.edu



**Fig 2:** Top: Reduction of **1** to **2**. Bottom Left: CV of **1** (3.0 mM **1**, 0.215 M [ $n\text{Bu}_4\text{N}$ ][PF<sub>6</sub>] in THF) collected at various scan rates and **2** (3.4 mM **2**, 0.271 M [ $n\text{Bu}_4\text{N}$ ][PF<sub>6</sub>] in THF) collected at a scan rate of 100 mV/s. All referenced to Fc<sup>0/+</sup> couple at 0.0 V. Bottom Right: Thermal ellipsoid plot of **2** (50% probability level) with hydrogen atoms (except for H1) and residual Et<sub>2</sub>O omitted for clarity.

Previously, our group reported the Ti<sup>IV</sup> imido complex [(Tp<sup>tBu,Me</sup>)Ti{≡NSi(CH<sub>3</sub>)<sub>3</sub>}(Cl)] (**1**) (Tp<sup>tBu,Me</sup> = hydridotris(3-*tert*-butyl-5-methylpyrazol-1-yl)borate) formed upon deazotation of (CH<sub>3</sub>)<sub>3</sub>SiN<sub>3</sub> by [(Tp<sup>tBu,Me</sup>)TiCl].<sup>16</sup> Cyclic voltammetry studies (CV) of **1** at slow scan rates (50 and 100 mV/s) revealed an irreversible reduction event at -2.32 V as well as an irreversible oxidation event at -1.53 V vs Fc<sup>0/+</sup>, **Fig 2** (blue trace). The latter oxidation feature becomes quasi-reversible at faster scan rates (≥150 mV/s, E<sub>1/2red</sub> = -1.61 V, E<sub>1/2ox</sub> = -1.53 V, **Fig 2**, red trace). These quasi-reversible features are dependent on the reduction event at -2.32 V and thus not observed in CV scans sweeping potentials >-1.9 V (see ESI for details). We initially assigned the reduction event at -2.32 V to a [(Tp<sup>tBu,Me</sup>)Ti{≡NSi(CH<sub>3</sub>)<sub>3</sub>}(Cl)]<sup>0/+</sup> redox couple, for which a subsequent chloride dissociation step leads to electrochemical irreversibility and the quasi-reversible features at -1.61/-1.53 V to a [(Tp<sup>tBu,Me</sup>)Ti{≡NSi(CH<sub>3</sub>)<sub>3</sub>}(THF)]<sup>+0</sup> redox couple. To probe this, 1-4 eq. [ $n\text{Bu}_4\text{N}$ ][Cl] were added to the electrolyte solution causing the quasi-reversible reduction event (-1.61 V) to disappear. This suggests a hypothetical cationic species such as “[(Tp<sup>tBu,Me</sup>)Ti{≡NSi(CH<sub>3</sub>)<sub>3</sub>}(THF)]<sup>+</sup>” to rapidly associate Cl<sup>-</sup> to form complex **1** with high concentrations of Cl<sup>-</sup>, however, when the chloride concentration is relatively low, it instead coordinates a PF<sub>6</sub><sup>-</sup> (See ESI and discussion below for details). It also suggests that the PF<sub>6</sub><sup>-</sup> coordinated “[(Tp<sup>tBu,Me</sup>)Ti{≡NSi(CH<sub>3</sub>)<sub>3</sub>}(THF)]<sup>+</sup>” is easier to reduce than **1** (*vide infra*). In any case, the reduction event at -2.32 V suggested the possibility of chemical reduction of **1** to a Ti<sup>III</sup> species, which, under electrochemical conditions, seemed unstable.

Accordingly, chemical reduction of **1** with one equivalent of KC<sub>8</sub> in THF yielded a yellow-brown microcrystalline material in 91% yield after work-up, identified as [(Tp<sup>tBu,Me</sup>)Ti{≡NSi(CH<sub>3</sub>)<sub>3</sub>}(THF)] (**2**), **Fig 2**, on the basis of structural and spectroscopic studies (*vide infra*). Room temperature <sup>1</sup>H-NMR spectroscopy revealed significantly broadened and paramagnetic shifts for the pyrazolyl, B-H, and trimethylsilyl resonances (ESI, **Fig S3.1.1**). Solution state magnetometry

determined *via* Evans method<sup>17</sup> (300 K in benzene-*d*<sub>6</sub>) revealed  $\mu_{\text{eff}} = 1.85 \mu_{\text{B}}$  consistent with a spin-only *d*<sup>1</sup> system.

Single crystal X-ray diffraction studies (scXRD) of **2**, **Fig 2**, revealed an unprecedented, terminally-bound, mononuclear Ti<sup>III</sup> imido with a short Ti≡NR length of 1.766(6) Å. The Ti≡NR bond length is only ~0.06 Å longer than the same metrical parameter found in the Ti<sup>IV</sup> precursor **1**, 1.692(1)-1.700(2) Å,<sup>16,18</sup> in line with the larger ionic radius of Ti<sup>III</sup> versus the more contracted Ti<sup>IV</sup> ion (0.67 vs 0.42 Å, respectively).<sup>19</sup> The Ti≡NR bond distance in **2** and the difference from its Ti<sup>IV</sup> analogue is in good agreement with the Ti≡NR bond distance of 1.770(4) Å and a difference of ~0.04 Å from its Ti<sup>IV</sup> analogue in the Ti<sub>2</sub><sup>III,III</sup> terminal imido reported by Bai *et al.*, **Fig 1B**.<sup>13</sup> The Ti≡NR bond length in complex **2** is however, longer than the terminal Ti≡NR bond distance of 1.729(3) Å reported recently by Gomez-Torres *et al.*<sup>15</sup> Additionally, the ∠Ti≡N-Si in **2** was found to be 172.6(4)°, which is more obtuse than the same angles of 158.94(10)-160.24(9)° found in precursor **1**.<sup>16,18</sup> We attribute the near-linear topology of the {Ti≡N-Si} core in **2** to the increase in the size of and change in geometry (**1**: τ<sub>5</sub> = 0.47-0.59, **2**: τ<sub>5</sub> = 0.29) about the Ti-center. The Ti-center in **2** lies an average of 0.17 Å further from the tris-pyrazole (NNN) plane (see ESI for details)<sup>16,18</sup> enabling the imido ligand to minimize steric repulsion with the bulky Tp<sup>tBu,Me</sup> ligand and become almost linear in **2**.

To better understand why **1** gave rise to two separate redox events and to determine if indeed the Cl<sup>-</sup> was interfering with reversibility, we collected CV data for **2**. We found that **2** possesses a fully reversible redox event at E<sub>1/2</sub> = -1.64 V vs Fc<sup>0/+</sup>, which we attribute to the Ti<sup>III</sup>/Ti<sup>IV</sup> redox couple, **Fig 2** (green trace in **Figs 2** and **S7.2.2**). No significant features were observed around -2.3 V (**Fig S7.2.3**). The reversible feature at -1.64 V for **2** coincides with the quasi-reversible oxidation/reduction peaks observed at -1.53/-1.61 V for **1** (*vide supra*), which suggests that one-electron oxidation of **2** to form a hypothetical “[**2**<sup>+</sup>][PF<sub>6</sub><sup>-</sup>]” salt becomes reversible when chloride ions are absent and ample [PF<sub>6</sub><sup>-</sup>] is present, and this suggests that “[(Tp<sup>tBu,Me</sup>)Ti{≡NSi(CH<sub>3</sub>)<sub>3</sub>}(THF)]<sup>+</sup>” is more easily reduced than **1** (see ESI for details). This feature also suggests that one-electron oxidation of **2** at the electrode surface to form hypothetical “[**2**<sup>+</sup>][PF<sub>6</sub><sup>-</sup>]” involves minimal reorganization energy due to the weakly coordinating nature of PF<sub>6</sub><sup>-</sup> unlike with Cl<sup>-</sup> (*vide supra*).

To better understand the electronic structure of **2**, we prepared a close structural and electronic analogue [(Tp<sup>tBu,Me</sup>)TiCl(OEt<sub>2</sub>)] [B(C<sub>6</sub>F<sub>5</sub>)<sub>4</sub>] (**3**<sup>Et<sub>2</sub>O</sup>) independently from oxidation of [(Tp<sup>tBu,Me</sup>)TiCl]<sup>16</sup> with [Ti][B(C<sub>6</sub>F<sub>5</sub>)<sub>4</sub>] in Et<sub>2</sub>O in 65.7% yield (ESI, Section 2.3). The THF complex, [(Tp<sup>tBu,Me</sup>)TiCl(THF)] [B(C<sub>6</sub>F<sub>5</sub>)<sub>4</sub>] (**3**<sup>THF</sup>), was analogously prepared but proved more challenging to purify. These cationic chloride complexes were chosen as close structural analogues of **2** to assess the perturbation of the electronic structure of the *d*<sup>1</sup> ion caused by the multiple bond character of the imido group and to assess the role of a dative solvent ligand. Akin to **2**, the solution magnetic susceptibility measurement of **3**<sup>Et<sub>2</sub>O</sup> yielded  $\mu_{\text{eff}} = 1.86 \mu_{\text{B}}$  at 300 K in THF-*d*<sub>8</sub> in agreement with a spin-only *d*<sup>1</sup> species. To further probe the electronic structure of **2**, we

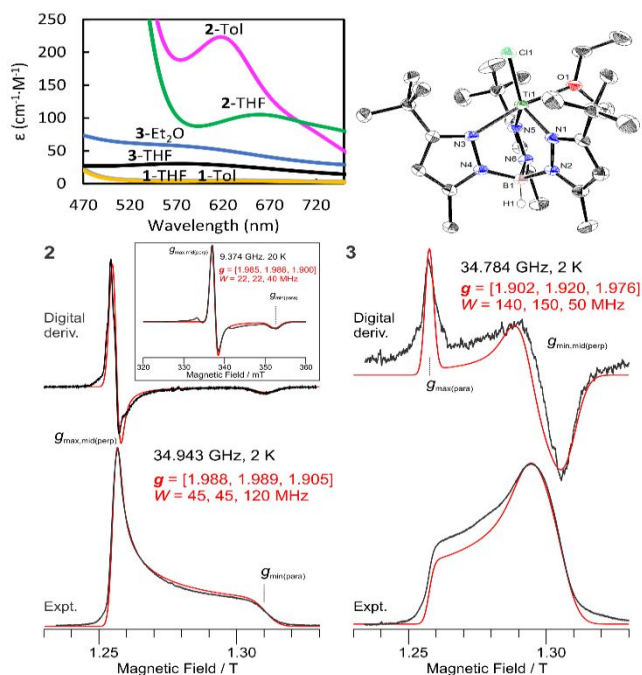


**Fig 3:** Top Left: UV-Vis spectrum of **1**, **2**, and **3** in solvents listed (Tol = toluene). Top Right: X-ray structure of **3Et<sub>2</sub>O** (50% probability level) with hydrogen atoms (except for H1), residual Et<sub>2</sub>O, and [B(C<sub>6</sub>F<sub>5</sub>)<sub>4</sub>]<sup>-</sup> omitted for clarity. Bottom Left: EPR spectra of **2** in Tol/THF frozen solution (black traces; simulations as red traces with  $S = 1/2$  parameters as shown). Main figure: Q-band (34.943 GHz, 2 K) spectrum. Experimental spectrum shown in absorption mode due to rapid passage effects. Digital derivative shown above for comparison with conventional (first derivative) EPR. Inset: X-band (9.374 GHz, 20 K) spectrum in first derivative (slow passage) mode. Bottom right: EPR spectrum of **3Et<sub>2</sub>O** in Tol frozen solution.

turned to UV-vis spectroscopy, **Fig 3**. The  $d^0$  precursor, **1**, unsurprisingly, displays no absorption bands in the range 500–750 nm (THF or toluene solvent, yellow and gray). In contrast, **2** and **3** each display a low-intensity feature consistent with a  $d-d$  transition (**Fig 3**): **2**: 618 nm ( $\epsilon = 225 \text{ cm}^{-1}\cdot\text{M}^{-1}$ , toluene, pink) and 659 nm ( $\epsilon = 110 \text{ cm}^{-1}\cdot\text{M}^{-1}$ , THF, green); **3** (**3<sup>THF</sup>**): 574 nm ( $\epsilon = 30 \text{ cm}^{-1}\cdot\text{M}^{-1}$ , THF, black) and (**3<sup>Et<sub>2</sub>O</sup>**): 584 nm ( $\epsilon = 56 \text{ cm}^{-1}\cdot\text{M}^{-1}$ , Et<sub>2</sub>O, blue). The solvent-dependence in the intensity and absorption energy for electronic transitions in complex **2** are consistent with dissociation of the THF ligand in toluene to form a putative four-coordinate Ti<sup>III</sup> imido [(Tp<sup>tBu,Me</sup>)Ti(=NSi(CH<sub>3</sub>)<sub>3</sub>)]. In a previous study, it was found that an isoelectronic V<sup>IV</sup> nitrido complex, [(Tp<sup>tBu,Me</sup>)V(=N)(THF)], readily expels THF in weakly coordinating solvents.<sup>20</sup> The near order of magnitude increase in molar absorptivity between **3** and **2** reflects the forbidden nature of  $d-d$  transitions occurring in **3** (selection rule for orbital quantum number:  $\Delta l = \pm 1$ ), versus the more allowed  $d_{xy} \rightarrow \pi^*_{\text{Ti=NR}}$  transitions in **2** (excitations to molecular orbitals with titanium and nitrogen parentage), which is consistent with the bonding and spectroscopic properties for a  $d^1$  systems having metal-ligand multiple bonds developed by Ballhausen and Gray for the isoelectronic vanadyl ion, {V=O}<sup>2+</sup>.<sup>12</sup>

Further spectroscopic evidence for the presence of a Ti-centric radical in **2** was obtained through continuous wave (CW) X- and Q-band EPR spectroscopy. Surprisingly, **2** exhibited an axial  $S = 1/2$  spectrum ( $g_{x(\text{max})} \approx g_{y(\text{mid})} \approx g_{\perp} > g_{z(\text{min})} = g$ ) in toluene and toluene/THF glasses, **Fig 3**, (X-band (insert), toluene

glass,  $g_{x,y,z} = [1.985, 1.986, 1.900]$ , 20 K; Q-band (main **Fig 3**), 1:1 (v/v) toluene/THF glass,  $g_{x,y,z} = [1.988, 1.989, 1.905]$ , 2 K) despite its low symmetry observed in the solid state by sXRD. The  $g$  values observed for **2** display a pattern similar to {V=O}<sup>2+</sup>, in which  $g_{\perp}$  is closer to  $g_e$  (2.00) than  $g$  due to the energetic ordering of the V 3d orbitals in triply-bonded {V=O}<sup>2+</sup>, and in line with the electronic structure of **2** being strongly defined by {Ti=NSiMe<sub>3</sub>} bonding.<sup>12,24</sup> This axial EPR, expected for a trigonally symmetric four-coordinate complex, is consistent with the results of UV-Vis spectroscopy in toluene, however, there is no change in X-band EPR between 1:1 THF:toluene glass and toluene glass (ESI, **Fig S6.1.2**). This indicates structural changes around the periphery of the {Ti=NR}<sup>+</sup> fragment have minimal effect on the magnetic properties of **2**. No hyperfine coupling to the imido nitrogen was detected indicating that the unpaired electron is metal centered and in a  $d$ -orbital orthogonal to the Ti=NR bond. In comparison, the EPR spectrum of **3<sup>Et<sub>2</sub>O</sup>** is also roughly axial, but with ( $g_{x(\text{min})} \approx g_{y(\text{mid})} \approx g_{\perp} < g_{z(\text{max})} = g$ ; Q-band,  $g_{x,y,z} = [1.902, 1.920, 1.976]$ , 2 K) and is thus similar, albeit less rhombic, to the neutral, five-coordinate complex [Tp<sup>tBu,Me</sup>Ti<sup>III</sup>Cl<sub>2</sub>].<sup>16</sup> We propose the EPR differences between **2** and **3** to result from the stronger  $\pi$ -donation of the imido compared to the chloride.<sup>21</sup> Further comparisons among EPR spectra of **3** are given in the ESI.

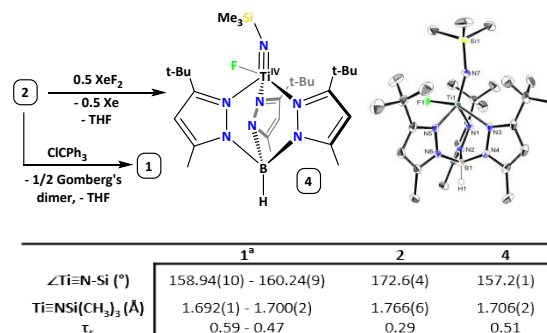


**Figure 4:** Top left: Reactivity of **2** with ClCPh<sub>3</sub> and XeF<sub>2</sub> to form **1** and **4** respectively. Bottom Top right: Thermal ellipsoid plot of **4** (50% probability level) with hydrogen atoms (except for H1) and residual Et<sub>2</sub>O omitted for clarity. Bottom: Table of the structural parameters of compounds **1**, **2**, and **4**. <sup>a</sup>Previously reported.<sup>16</sup>

Taking advantage of the radical nature of **2**, we chemically probed its electrochemical features (*vide supra*); oxidation of **2** with ClCPh<sub>3</sub> quantitatively formed **1** along with Gomberg's dimer as evidenced by <sup>1</sup>H-NMR spectroscopy (Fig S3.2.1).<sup>22</sup> In an attempt to desilylate **2** with 0.5 eq. of XeF<sub>2</sub>, we instead observed the formation of the imido-fluoride [(Tp<sup>tBu,Me</sup>)Ti(=NSi(CH<sub>3</sub>)<sub>3</sub>)(F)] (**4**), in 86% yield, **Fig 4**. Complex **4** is resistant to FSiMe<sub>3</sub> elimination even under forcing conditions (70 °C, 18 hrs) and metrically, the structures of **1** and **4** are quite similar (Table in **Fig 4**). The room temperature <sup>19</sup>F-NMR spectrum of **4** exhibits one sharp resonance at +131.4 ppm, and unlike **1**, complex **4** undergoes rapid Berry pseudo-rotation on the NMR time scale (300 K) resulting in equivalent pyrazolyl moieties in solution (ESI, **Fig S3.4.1**).<sup>23</sup>

We have provided conclusive evidence for the synthesis of the first mononuclear, Ti<sup>III</sup> complex containing a terminal imido ligand, {Ti=NSi(CH<sub>3</sub>)<sub>3</sub>}<sup>+</sup>. Electrochemical and chemical

reversibility of the interconversion between Ti<sup>IV</sup> imido **1** and Ti<sup>III</sup> imido **2** were probed by CV, reduction with potassium graphite, and oxidation with ClCPh<sub>3</sub>. We observed no evidence for desilylation of the trimethylsilylimido upon treatment of the Ti<sup>III</sup> center with an electrophilic fluoride source (XeF<sub>2</sub>) and instead form a {Ti-F}<sup>3+</sup> unit, **4**. In probing the radical nature of **2**, we provided evidence from EPR of a Ti-centered radical having axial symmetry, where the unpaired electron resides in a d-orbital perpendicular to the orbitals involved in  $\pi$ -donation from the imido ligand which resembles the well-known vanadyl unit, {V=O}<sup>2+</sup>. The EPR behavior of **2** contrasts with that of **3**, which contains only a {Ti-Cl}<sup>2+</sup> unit. This work demonstrates the synthetic accessibility of a mononuclear Ti<sup>III</sup> terminal imido which may show great synthetic utility like its diamagnetic Ti<sup>IV</sup> predecessors.

### Conflicts of interest

There are no conflicts to declare.

### Acknowledgements

The authors wish to acknowledge Amy Metlay and Dr. Rolando Aguilar for helpful discussions surrounding the structure and electrochemistry of **2**. D.J.M. thanks the U.S. National Science Foundation (NSF; Grants CHE-0848248 and CHE-1152123) and the University of Pennsylvania for funding and J.T. also thanks the NSF (Grant MCB-1908587) for support. We thank Prof. Brian M. Hoffman (Northwestern University, Evanston, IL) for use of EPR spectrometers supported by the NIH (grant GM-111097).

### Notes and references

- (a) P. J. Walsh, F. J. Hollander and R. G. Bergman, *J. Am. Chem. Soc.*, **1988**, 110, 8729-8731. (b) E. W. Harlan and R. H. Holm, *J. Am. Chem. Soc.*, **1990**, 112, 186-193. (c) P. Legzdins, E. C. Phillips, S. J. Rettig, J. Trotter, J. E. Veltheer and V. C. Yee, *Organometallics*, **1992**, 11, 3104-3110. (d) V. C. Gibson, C. Redshaw, W. Clegg and M. R. J. Elsgood, *J. Chem. Soc., Chem. Commun.*, **1994**, 2635. (e) D. L. Morrison and D. E. Wigley, *Inorg. Chem.*, **1995**, 34, 2610-2616. (f) J. I. Fostvedt, L. N. Grant, B. M. Kriegel, A. H. Obenhuber, T. D. Lohrey, R. G. Bergman and J. Arnold, *Chem. Sci.*, **2020**, 11, 11613-11632.
- (a) W. A. Nugent and B. L. Haymore, *Coord. Chem. Rev.*, **1980**, 31, 123-175. (b) S. M. Rocklage, R. R. Schrock, M. R. Churchill and H. J. Wasserman, *Organometallics*, **1982**, 1, 1332-1338. (c) T. R. Cundari, *J. Am. Chem. Soc.*, **1992**, 114, 7879-7888. (d) R. R. Schrock and A. H. Hoveyda, *Angew. Chem., Int. Ed.*, **2003**, 42, 4592-4633. (e) K. Kawakita, B. F. Parker, Y. Kakiuchi, H. Tsurugi, K. Mashima, J. Arnold and I. A. Tonks, *Coord. Chem. Rev.*, **2020**, 407, 213118.
- (a) G. Tejada, D. S. Belov, D. A. Fenoll, K. L. Rue, C. Tsay, X. Solans-Monfort and K. V. Bukhryakov, *Organometallics*, **2022**, 41, 361-365. (b) Y. Jin, Y. Yang, C. Su, J. Wang, Y. Wang and B. Liu, *Macromol. React. Eng.*, **2022**, 16, 2200025. (c) N. A. H. Male, M. E. G. Skinner, S. Y. Bylikin, P. J. Wilson, P. Mountford and M. Schröder, *Inorg. Chem.*, **2000**, 39, 5483-5491. (d) N. Adams, H. J. Arts, P. D. Bolton, D. Cowell, S. R. Dubberley, N. Friederichs, C. M. Grant, M. Kranenburg, A. J. Sealey, B. Wang, P. J. Wilson, A. R. Cowley, P. Mountford and M. Schröder, *Chem. Commun.*, **2004**, 434-435. (e) J. Jin, W. R. Mariott and E. Y. X. Chen, *J. Polym. Sci., Part A: Polym. Chem.*, **2003**, 41, 3132-3142.
- (a) S. M. Pugh, D. J. M. Trösch, D. J. Wilson, A. Bashall, F. G. N. Cloke, L. H. Gade, P. B. Hitchcock, M. McPartlin, J. F. Nixon and P. Mountford, *Organometallics*, **2000**, 19, 3205-3210. (b) A. E. Guiducci, C. L. Boyd and P. Mountford, *Organometallics*, **2006**, 25, 1167-1187. (c) A. J. Blake, J. M. McInnes, P. Mountford, G. I. Nikonov, D. Swallow and D. J. Watkin, *J. Chem. Soc., Dalton Trans.*, **1999**, 379-392.
- (a) S. P. Heins, P. T. Wolczanski, T. R. Cundari and S. N. Macmillan, *Chem. Sci.*, **2017**, 8, 3410-3418. (b) P. L. McGrane and T. Livinghouse, *J. Am. Chem. Soc.*, **1993**, 115, 11485-11489. (c) T. E. Hanna, I. Keresztes, E. Lobkovsky, W. H. Bernskoetter and P. J. Chirik, *Organometallics*, **2004**, 23, 3448-3458.
- Y. Li, Y. Shi and A. L. Odom, *J. Am. Chem. Soc.*, **2004**, 126, 1794-1803.
- (a) M. Fischer, M. Manßen, M. Schmidtman, T. Klüner and R. Beckhaus, *Chem. Sci.*, **2021**, 12, 13711-13718. (b) C. C. Cummins, C. P. Schaller, G. D. Van Duyne, P. T. Wolczanski, A. W. E. Chan and R. Hoffmann, *J. Am. Chem. Soc.*, **1991**, 113, 2985-2994.
- (a) Z. W. Davis-Gilbert, L. J. Yao and I. A. Tonks, *J. Am. Chem. Soc.*, **2016**, 138, 14570-14573. (b) Z. W. Gilbert, R. J. Hue and I. A. Tonks, *Nat. Chem.*, **2016**, 8, 63-68.
- (a) B. M. Hoffman, D. Lukoyanov, Z.-Y. Yang, D. R. Dean and L. C. Seefeldt, *Chem. Rev.*, **2014**, 114, 4041-4062. (b) C. Lorber, *Coord. Chem. Rev.*, **2016**, 308, 76-96. (c) N. Hazari and P. Mountford, *Acc. Chem. Res.*, **2005**, 38, 839-849.
- (a) D. C. Bradley and E. G. Torrible, *Can. J. Chem.*, **1963**, 41, 134-138. (b) N. W. Alcock, M. Pierce-Butler and G. R. Willey, *J. Chem. Soc., Chem. Commun.*, **1974**, 627a-627a.
- J. E. Hill, R. D. Profilet, P. E. Fanwick and I. P. Rothwell, *Angew. Chem., Int. Ed.*, **1990**, 29, 664-665.
- C. J. Ballhausen and H. B. Gray, *Inorg. Chem.*, **1962**, 1, 111-122.
- G. Bai, P. Wei and D. W. Stephan, *Organometallics*, **2006**, 25, 2649-2655.
- H. Tsurugi, H. Nagae and K. Mashima, *Chem. Commun.*, **2011**, 47, 5620-5622.
- A. Gómez-Torres, N. Mavragani, A. Metta-Magaña, M. Murugesu and S. Fortier, *Inorg. Chem.*, **2022**, 61, 16856-16873.
- A. Reinholdt, D. Pividori, A. L. Laughlin, I. M. DiMucci, S. N. MacMillan, M. G. Jafari, M. R. Gau, P. J. Carroll, J. Krzystek, A. Ozarowski, J. Telser, K. M. Lancaster, K. Meyer and D. J. Mindiola, *Inorg. Chem.*, **2020**, 59, 17834-17850.
- (a) D. F. Evans, *J. Chem. Soc.*, **1959**, 2003-2005. (b) S. K. Sur, *J. Mag. Res. (1969)*, **1989**, 82, 169-173. (c) G. A. Bain and J. F. Berry, *J. Chem. Ed.*, **2008**, 85, 532.
- A range for the Ti-imido bond distances in **1** is presented as three inequivalent molecules of **1** make up the unit cell of **1** as previously reported.
- R. D. Shannon, *Acta Cryst. A*, **1976**, 32, 751-767.
- M. G. Jafari, D. Fehn, A. Reinholdt, C. Hernández-Prieto, P. Patel, M. R. Gau, P. J. Carroll, J. Krzystek, C. Liu, A. Ozarowski, J. Telser, M. Delferro, K. Meyer and D. J. Mindiola, *J. Am. Chem. Soc.*, **2022**, 144, 10201-10219.
- V. C. Gibson, *J. Chem. Soc., Dalton Trans.*, **1994**, 1607-1618.
- M. Gomberg, *J. Am. Chem. Soc.*, **1900**, 22, 757-771.
- (a) C. Serre, T. Corbière, C. Lorentz, F. Taulelle and G. Férey, *Chem. Mater.*, **2002**, 14, 4939-4947. (b) R. S. Berry, *J. Chem. Phys.*, **1960**, 32, 933-938.
- D. Baute, D. Goldfarb, *J. Phys. Chem. A*, **2005**, 109, 7865-7871